Comparative Study of MPPT Controllers for a Wind Energy Conversion System

Hamid Chojaa[1(✉)], Aziz Derouich[1], Yassine Bourkhime[2], Elmostafa Chetouani[3], Billel Meghni[4], Seif Eddine Chehaidia[5], and Mourad Yessef[6]

[1] Laboratory of Technologies and Industrial Services, Higher School of Technology, Sidi Mohamed Ben Abdellah University, 30000 Fez, Morocco
hamid.chojaa@usmba.ac.ma
[2] National School of Applied Sciences, Abdelmalek Essaâdi University, Tetouan, Morocco
[3] Laboratory: Electronics, Instrumentation and Energy, Faculty of Science, University Chouaib Doukkali, Eljadida, Morocco
[4] Engineering Department, LSEM Laboratory, University of Badji Mokhtar, Annaba, Algeria
[5] Research Laboratory of Industrial Risks, Non Destructive Control and Operating Safety, University of Badji Mokhtar, Annaba, Algeria
[6] Laboratory of Engineering, Modeling and Systems Analysis, SMBA University, Fez, Morocco

Abstract. This paper aims to discuss the modeling and control of a wind turbine using the maximum power point tracking technique (MPPT) based on the Tip Speed Ratio (TSR) method to extract the maximum power. A comparative study has been carried out within a four-types control laws. Namely, conventional PI, nonlinear sliding mode, backstepping and finally, artificial neural network controller. To identify which is which to provide the best performances, the proposed control laws are tested under Matlab/Simulink under different operating conditions to check the controller's performances. The performed simulations show that MPPT artificial neural network ensure the best performance compared to other controller because of its ability to map between inputs and outputs and efficiently cope with wind energy conversion system (WECS) nonlinearities.

Keywords: MPPT · Artificial neural network control · Sliding mode control · Backstepping control

1 Introduction

The traditional energy sources have become more dangerous and threatening for both the planet and humanity because of its harmful environmental impact. Hence, the sustainable green energy has gained attention as a clean energies vector avoiding the global warming, through the reduction of polluting gas emissions. There are several kinds of renewable energies, which are promising alternatives to the fossil energy, among these the wind energy is considered as one of the best alternatives to solve this issue. WECS can transform the kinetic energy to mechanical energy and then to electrical energy through the choice of the appropriate to feed the grid [1–3].

R. Saidi et al. (Eds.): ICATH 2021, LNDECT 110, pp. 300–310, 2022.
https://doi.org/10.1007/978-3-030-94188-8_28

The variable speed wind power system based on the Doubly Feed Induction Generator (DFIG) is widely used in onshore wind farms [4–6]. The latest progress in renewable energies proves that the configuration in WECS shown in Fig. 1 is the most demanding for electrical energy production [7]. It allows to extract the power in a wide speed range with a flexible control which reduces the power/cost ratio and the advantages of which are more convincing [8]. The DFIG allows operation over a speed range of ±33% around the synchronous speed, thus guarantee a simple converters configuration and gives more flexibility to control system and task. Consequently, reduce the cost the produced energy [9].

A WECS is a highly nonlinear system, characterized by sudden variations in wind speed. Then the use of an MPPT strategy is essential to improve the extraction of kinetic power from the wind in the wide range of wind speed. The MPPT controllers used to reach and track the MPPT available in the wind by regulating the rotor speed [1, 2].

The aim of this paper is to elaborate and compare serval MPPT control laws; four types of control are proposed to ensure a good rotor speed regulation and mechanical load mitigation. The presented control techniques are respectively:

- PI linear control,
- nonlinear sliding mode control (SMC),
- nonlinear Backstepping control (BAC),
- Artificial neural network (ANN).

This work will be organized as follows: the next part describes the WENCS modeling, then the proposed control strategies are presented. Main results are presented and discussed in Sect. 4 and finally, the conclusion.

2 WECS Modeling

The aerodynamic behavior of wind turbine is the first interesting element in the conversion chain. It used to convert the kinetic power into mechanical one. Therefore, aerodynamic modeling is a key element in the WECS. Its known by its nonlinearity, which requires advanced identification, modeling or estimation technics [3]. Many researchers use different kinds of models according to the wind turbine in use. In the present manuscript, a popular useful model, derived from the reference herein is used [2, 4] WECS based DFIG supplies a grid load through the following chain: aerodynamic wind turbine rotor, gearbox, DFIG, rectifier, and an inverter. Wind turbine converts the kinetic energy to mechanical energy, the gearbox multiplies the rotor speed in order to reach the generation condition and produce electrical energy.

The generated power is given by [2]:

$$P_t = \frac{1}{2}\rho\pi R^2 V^3 C_P(\lambda, \beta) \tag{1}$$

In this work, the variations of $Cp(\lambda, \beta)$ are modeled by [2, 4]:

$$\begin{cases} Cp(\lambda, \beta) = 0.5\left(\frac{116}{\lambda i} - 0.4\beta - 5\right)exp\left(\frac{-21}{\lambda i}\right) + 0.0068\lambda \\ \frac{1}{\lambda i} = \frac{1}{\lambda + 0.08\beta} - \frac{0.035}{\beta^3 + 1}; \qquad \lambda = \frac{\Omega_t R}{V} \end{cases} \tag{2}$$

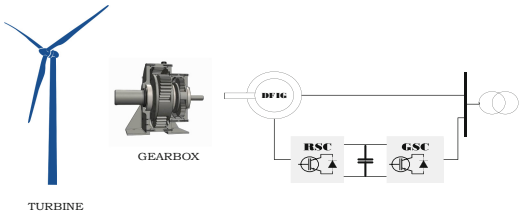

Fig. 1. The WECS based on DFIG.

By applying the fundamental equation of dynamic, one gets:

$$J\frac{d\Omega_g}{dt} = C_{méc} = C_g - C_{em} - C_f \tag{3}$$

Where the C_{em} is the electromechanical torque of generator. We notice that the electromechanical torque is presented as a resistive torque for all system and C_f is proportional to rotational speed of shaft and that is given by (4), such us:

$$C_f = f_v\Omega_g \tag{4}$$

Applying again the Laplace transform (3), we can find the transfer function representing wind turbine mechanical system as shown below:

$$\Omega g(s) = (Cg - Cem)\left(\frac{1}{J.s + fv}\right) \tag{5}$$

Finally, the global model of a wind turbine will be achieved by adding all parts of the transmission chain models and that lead to representing bloc diagram as shown in Fig. 2.

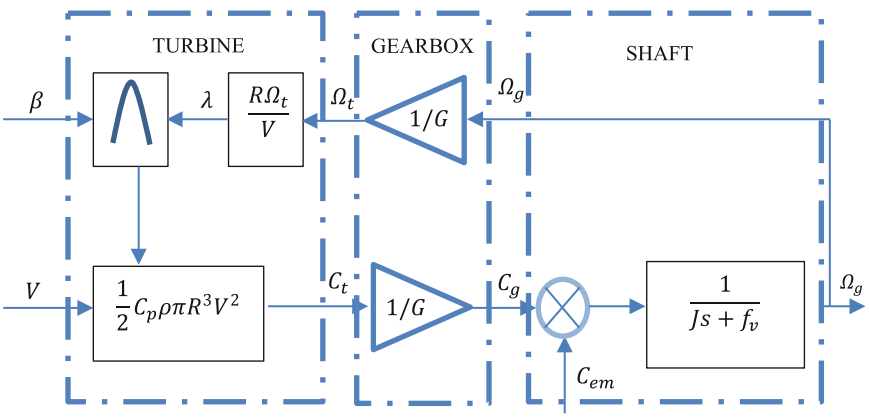

Fig. 2. Global model for mechanical transmission chain

3 MPPT Based TSR Method

In this paper, The MPPT technique has been realized with mechanical speed control as shown in Fig. 3. This control strategy consists of adjusting the electromagnetic torque that is developed by the electrical generator in order to fix it at its reference value. In the next, we present four controllers, being mentioned in Sect. 1, designed to track the generator reference speed $\Omega g*$ according to maximum power value.

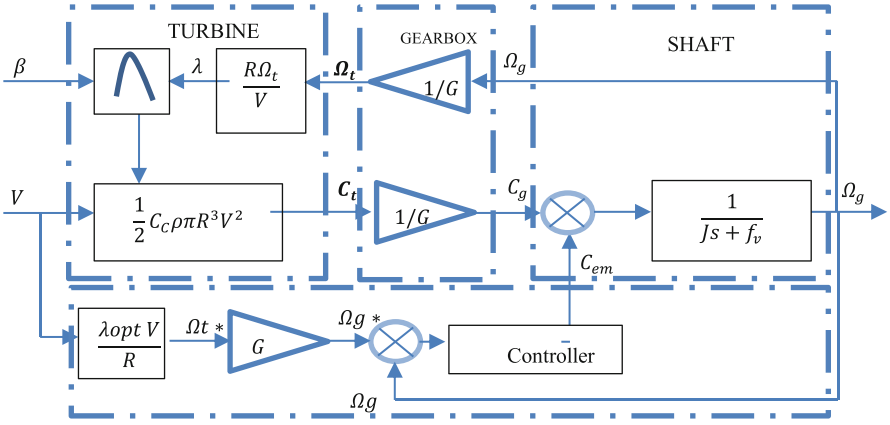

Fig. 3. MPPT technique with speed controller.

3.1 PI Controller

The PI controller is the most popular controller in the industry because of its efficiency and practical implementation; unfortunately, it's less robust and instable in some use circumstances. The PI controller is used in close loop to correct the mechanical transfer function performances parameters such as stability, response time and precision. In most case the choosing factors Kp and Ki depend on the use conditions and preferable performance to respect. To apply this controller the knowledge of the system parameters is required to reach the best results and the best system performances. Figure 4 shows the block scheme for the implementation of the PI controller applied to mechanical shaft equation in close loop.

The closed-loop transfer function is written:

$$\frac{\Omega_{g(s)}}{\Omega_{g^*(s)}} = \frac{2\xi.\omega_n.s + \omega_n^2}{s^2 + 2\xi.\omega_n.s + \omega_n^2} = \frac{\frac{K_i + K_p.S}{J}}{s^2 + \frac{K_p.f_v}{J}.s + \frac{K_i}{J}} \tag{6}$$

The parameters K_p and K_i of the PI controller are given by the expressions:

$$\begin{cases} K_p = 2\xi.\omega_n.J - f_V \\ K_i = J.\omega_n^2 \end{cases} \tag{7}$$

The parameters K_p and K_i can be identified by solving the equality of equation above, where the ω_n and ξ is choosing by user according to preferable operating mode.

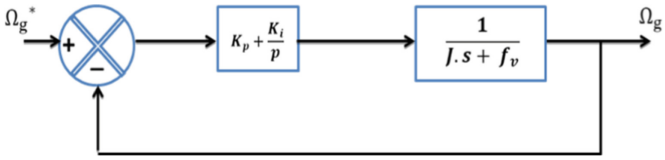

Fig. 4. Typical regulator PI structure.

3.2 Backstepping Controller

The Backstepping methodology can be defined as a way of division of a given system into several cascading subsystems. Based on sliding mode theory, all subsystem has to reach an intrinsic sliding surface, then, maintain the sliding state in order to achieve a global convergence. A control law stabilizing the system is derived from a Lyapunov function to prove the stability of the synthetized control law [6].

One of the advantages provided by the Backstepping method is its ability to keep the properties of the initial system in the synthetized control law. This is in a way the peculiarity of Backstepping compared to other methods [7]. Passivity is linked to other very important concepts such as stability, detectability and optimality. All these notions are necessary for the synthesis of the control laws. For the beign cited reasons, the analysis begins with the study of the Backstepping method to lead to its application to strict-feedback systems. In our study, to design a backstepping speed control, we have to start from the dynamic's equation and define the tracking error of the set point.

$$e(\Omega_g) = \Omega_g^* - \Omega_g \tag{8}$$

We consider the following Lyapunov function:

$$v(e) = \frac{1}{2} e(\Omega_g)^2 \tag{9}$$

The Lyapunov function derivative:

$$\dot{v}(e) = e(\Omega_g).\dot{e}(\Omega_g) = e(\Omega_g).\left(\dot{\Omega}_g^* + \frac{1}{J}(C_{em} + f_v.\Omega_g - C_g)\right) \tag{10}$$

The stabilizing control of backstepping is defined as follows:

$$C_{em}^* = -J.\dot{\Omega}_g^* - f_v.\Omega_g + C_g - K_1.e(\Omega_g) \tag{11}$$

With: K_1 positive constant.
We replace the expression (11) in (10) we get:

$$\dot{v}(e) = -K_1.e(\Omega_g)^2 < 0 \tag{12}$$

To ensure system's stability, the condition above must be verified.

3.3 Sliding Mode Controller

The sliding mode control is a variable structure nonlinear control method. The control structure is designed, keeping as primary objective, all system trajectories converge to an desired hypersurface. In our case the application of SMC it done with only one variable which means the application is reduced to a scalar variable C_{em} considered as tracking variable. To make appear the command C_{em}^{*}, the relative degree of the surface is equal to one. The sliding surface is defined by:

$$S(\Omega_g) = \Omega_g^{*} - \Omega_g \tag{13}$$

By Applying the following Lyapunov function to slide variable:

$$V(S(\Omega_g)) = \frac{1}{2}S(\Omega_g)^2 \tag{14}$$

The Lyapunov function derivative:

$$\dot{V}(S(\Omega_g)) = S(\Omega_g).\dot{S}(\Omega_g) \tag{15}$$

With: $\dot{S}(\Omega_g) = \dot{\Omega}_g^{*} - \dot{\Omega}_g$

By combining the above expressions in the last equations, we can write:

$$\dot{S}(\Omega_g) = \dot{\Omega}_g^{*} + \frac{1}{J}(C_{em} + f_v.\Omega_g - C_g) \tag{16}$$

Replacing the expression of C_{em} by the equivalent commands $(C_{emeq} + C_{emn})$ in Eq. (16) we find:

$$\dot{S}(\Omega_g) = \dot{\Omega}_g^{*} + \frac{1}{J}((C_{emeq} + C_{emn}) + f_v.\Omega_g - C_g) \tag{17}$$

In steady state we have: $S(\Omega_g) = 0$; $\dot{S}(\Omega_g) = 0$ and $C_{emn} = 0$, from which we extract the expression of the equivalent command C_{emeq}:

$$C_{emeq} = -J.\dot{\Omega}_g^{*} - f_v.\Omega_g + C_g \tag{18}$$

Replacing in the expressions above gives:

$$\dot{S}(\Omega_g) = \frac{1}{J}C_{emn} \tag{19}$$

To ensure the convergence of Lyapunov's function, we set:

$$C_{emn} = -K_2.\text{sign}(S(\Omega_g)) \tag{20}$$

With: K_2 positive constant.

3.4 Artificial neural networks Controller

In our paper, the MPPT neural networks controller was selected as a static Multi-Layers Perceptron (MLP). The Fig. 5 illustrate the architectural scheme of the used MLP [2, 10]. The proposed controller was composed of an input layer with two neurons, which were mechanical speed and its reference, two hidden layers, with 20 and 10 neurons respectively, an output layer with one neuron, which represents the generated reference torque. The curve of training and test is shown in Fig. 6.

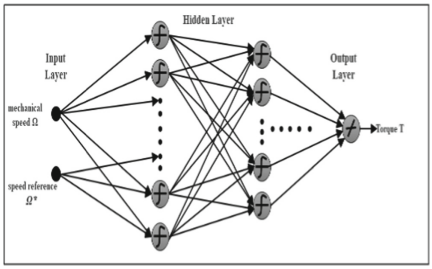

Fig. 5. ANN controller concept MLP.

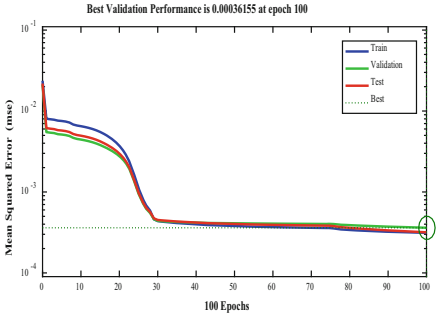

Fig. 6. Training and test performance curves.

4 Results and Discussions

In this section, the performance of the proposed controllers is evaluated and compared in terms of the reference tracking, static error, the dynamic response, system stability and robustness. The overall system considering a wind turbine which has been simulated using Matlab/Simulink, main parameters of the used wind turbine are summirized in Table 1. In addition, for a valuable validation of the proposed control methodologies, two different wind speed scenarios has been applied.

Table 1. Parameters of the used wind turbine

Parameters	Value
Volume density of the air ρ	1.225 $\frac{\text{Kg}}{\text{m}^3}$
Number of blades	3
Blade radius R	2 m
Pitch angle β	0°

4.1 Robustness Tests

For the best performance evaluation, a robustness test should be carried out on the different control techniques in order to evaluate their respective merit for a radical change in the wind profile as shown in Figs. 7. Figures 8, 9 and 10 shows the evolution of the four MPPT methods with mechanical speed control. Considering variable step wind speed scenario, one can clearly observe that the dynamic performance of the system based on ANNC is very efficient compared to other controllers SMC, PI and BAC. Under these variants conditions, the power coefficient C_p takes a maximum value of $C_{p\text{-max}} = 0.48$ for a pitch angle fixed at its minimum value, $\beta = 0°$.

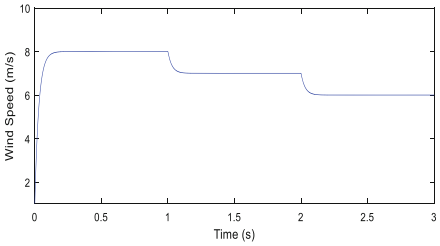

Fig. 7. Wind speed profile

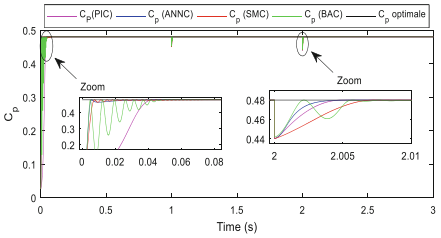

Fig. 8. Power coefficient

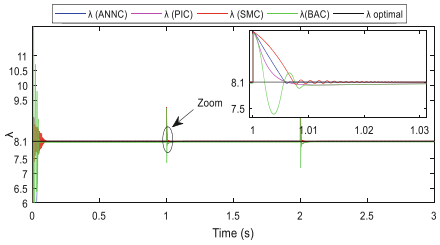

Fig. 9. Tip speed ratio.

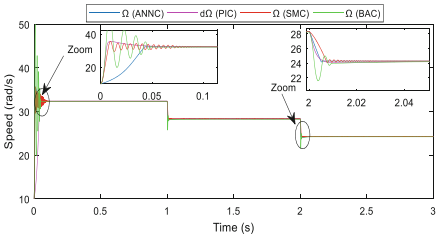

Fig. 10. Mechanical speed.

4.2 Tracking Tests

In this test the wind profile varies between 6 (m/s) and 10.5 (m/s) as shown in Fig. 11. To extract the maximum of the generated power, the speed ratio was set to the value $\lambda_{opt} = 8.1$, which corresponds to the maximum power coefficient $C_{p\text{-max}} = 0.48$ for any variation in wind speed. The results of the MPPT simulation with mechanical speed control by the four proposed controllers (PIC, SMC, BAC, ANNC) show clearly that for each value of wind speed, the mechanical speeds are perfectly following their references for the four MPPT methods with a significant static error for the BAC controller as we can see in Fig. 12. Similarly, it is observed that the ANN controller and SMC methods quickly achieve the static regime with a response time $T_s = 40$ (ms) and a negligible static error. On the other hand, the PI controller and Backstepping controller present a slightly slow response of about 60 (ms) in the dynamics regime with small fluctuations for the BAC controller and a negligible error for the PI controller (Fig. 13).

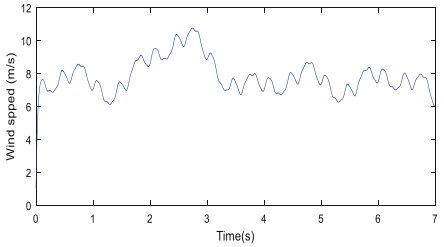

Fig. 11. Wind speed profile

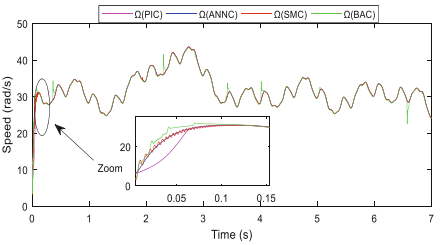

Fig. 12. Mechanical speed.

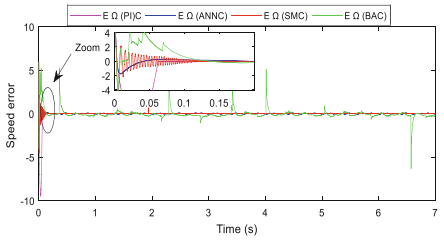

Fig. 13. Speed error.

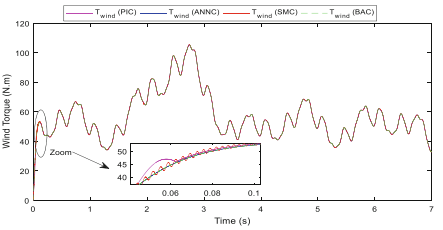

Fig. 14. Aerodynamic torque

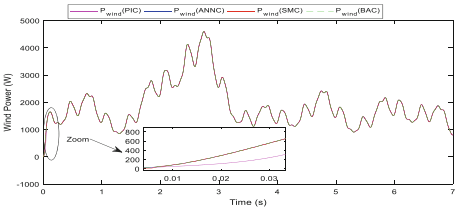

Fig. 15. Mechanical power.

Figures 14 and 15 show that in the four methods, the aerodynamic torque and the mechanical power follow their desired trajectories with a different efficiency. From the analysis of the results, it appears that the ANNC, and BAC present better performance in terms of response time and set point tracking.

The Table 2 below represents a synthesis of the comparison between the PIC, BAC, SMC and ANNC in term of the response time, set point tracking and static error. This table shows remarkable improvements obtained by ANNC. These improvements include an optimization of the static error, response time, set point tracking and robustness.

Table 2. Comparative result between the PIC, BAC, SMC and the ANNC.

Performance	PI	BAC	SMC	ANNC
Response time (s)	0.041	0.020	0.015	**0.0035**
Static errors (%)	0.241	0.175	0.198	**0.103**
Set-point tracking	Medium	Good	Very Good	**Very Good**
Robustness	Not Robust	Robust	Robust	**Robust**

5 Conclusion

This paper presents a comparative analysis of four MPPT control strategy using TSR method for controlling a variable speed wind turbine driven DFIG under low wind speed conditions. The compared controllers are: a conventional PI, BAC, SMC and ANNC. The study shows that the application of the ANNC MPPT control provides better speed regulation performance compared to other controllers, its allows a several advantages such as good tracking of references, robustness, a significant reduction in torque ripples, and faster dynamic response. In conclusion, the use of the ANNC results in the best and efficient control to tracking power.

References

1. Xiong, L., Li, P., Ma, M., Wang, Z., Wang, J.: Output power quality enhancement of PMSG with fractional order sliding mode control. Electr. Power Energy Systems **115** (2020)
2. Chojaa, H., Derouich, A., Chehaidia, S.E., Zamzoum, O., Taoussi, M., Elouatouat, H.: Integral sliding mode control for DFIG based WECS with MPPT based on artificial neural network under a real wind profile. Energy Rep. **7**, 4809–4824 (2021). https://doi.org/10.1016/j.egyr.2021.07.066
3. Zamzoum, O., El, Y., Errouha, M., Derouich, A., El, A.: Active and reactive power control of wind turbine based on doubly fed induction generator using adaptive sliding mode approach. Int. J. Adv. Comput. Sci. Appl. **10** (2019). https://doi.org/10.14569/IJACSA.2019.0100252
4. Hamid, C., Derouich, A., Taoussi, M., Zamzoum, O., Hanafi, A.: An improved performance variable speed wind turbine driving a doubly fed induction generator using sliding mode strategy. In: 2020 IEEE 2nd International Conference on Electronics, Control, Optimization and Computer Science (ICECOCS), pp. 1–8 (2020). https://doi.org/10.1109/ICECOCS50124.2020.9314629
5. Chojaa, H., Derouich, A., Taoussi, M., Zamzoum, O., Yessef, M.: Optimization of DFIG wind turbine power quality through adaptive fuzzy control. In: Motahhir, S., Bossoufi, B. (eds.) ICDTA 2021. LNNS, vol. 211, pp. 1235–1244. Springer, Cham (2021). https://doi.org/10.1007/978-3-030-73882-2_113
6. Meghni, B., Chojaa, H., Boulmaiz, A.: An optimal torque control based on intelligent tracking range (MPPT-OTC-ANN) for permanent magnet direct drive WECS. In: 2020 IEEE 2nd International Conference on Electronics, Control, Optimization and Computer Science (ICECOCS), pp. 1–6 (2020). https://doi.org/10.1109/ICECOCS50124.2020.9314304
7. Fdaili, M., Essadki, A., Nasser, T.: Comparative analysis between robust SMC & conventional PI controllers used in WECS based on DFIG. Int. J. Renew. Energy Res. **7**, 2151–2161 (2017)

8. Chehaidia, S.E., Abderezzak, A., Kherfane, H., Boukhezzar, B., Cherif, H.: An improved machine learning techniques fusion algorithm for controls advanced research turbine (Cart) power coefficient estimation. UPB Sci. Bull. Ser. C: Electr. Eng. Comput. Sci. **82**, 279–292 (2020)
9. Morshed, M.J., Fekih, A.: Integral terminal sliding mode control to provide fault ride-through capability to a grid connected wind turbine driven DFIG. In: 2015 IEEE International Conference on Industrial Technology (ICIT), pp. 1059–1064 (2015). https://doi.org/10.1109/ICIT.2015.7125237
10. Chehaidia, S.E., Abderezzak, A., Kherfane, H., Guersi, N., Cherif, H., Boukhezzar, B.: Fuzzy gain scheduling of pi torque controller to capture the maximum power from variable speed wind turbines. In: 2020 IEEE 2nd International Conference on Electronics, Control, Optimization and Computer Science, ICECOCS 2020 (2020)